sustainability

MDPI

Article

Characterization of Microalgae-Derived Alginate-like Expolymers (ALEs) and Their Crop-Promoting Effects and Resourcefulness

Yang Xiao, Fan Yi, Sudan Lin, Lin Li and Xueqing Shi *

School of Environmental and Municipal Engineering, Qingdao University of Technology, Qingdao 266520, China
* Correspondence: shixq@qut.edu.cn; Tel.: +86-18253220953

Abstract

This study selected the typical eutrophication associated algae species *Chlorella pyrenoidosa* and *Microcystis aeruginosa*, from which alginate-like expolymers (ALEs) were extracted. Their composition, structural characteristics, and potential as biofertilizers were systematically analyzed. Results indicate that both *C. pyrenoidosa-ALE* (Cp-ALE) and *M. aeruginosa*-ALE (Ma-ALE) primarily comprise proteins and polysaccharides as functional components. Cp-ALE exhibited higher extraction yields (35.34 ± 4.32 mg·g^{-1} VSS, volatile suspended solids) and richer growth-promoting constituents such as tryptophan, while Ma-ALE demonstrated higher aromaticity in its structure. Pot experiments further demonstrated that both ALEs exhibited a "low-concentration promotion, high-concentration inhibition" effect on ryegrass growth: at the optimal concentration (1:10,000), Cp-ALE and Ma-ALE increased ryegrass dry weight by 61.2% and 59.8%, respectively, with no significant difference compared to the algal whole-cell fertilizer (CF). This study has established a simple, environmentally friendly pathway for resource utilization of microalgal waste. Extracting ALEs effectively preserves plant-promoting components within microalgae, providing not only a sustainable solution for high-value utilization of eutrophication associated algae, but also a viable pathway for green agriculture and circular economic development.

Keywords: microalgae; alginate-like expolymers (ALEs); microalgae-derived fertilizer; circular economy; waste valorization; sustainable agriculture; concentration effect

1. Introduction

With the development of global industry and agriculture, nutrients such as nitrogen and phosphorus are constantly introduced into water bodies, accelerating the process of eutrophication and inducing explosive proliferation of microalgae and algal blooms. This issue has posed a severe challenge to global ecological sustainability [1,2]. If algal biomass is improperly managed after harvesting or natural decay, it will release nutrients such as nitrogen and phosphorus during decomposition, resulting in a vicious circle of water pollution. Furthermore, toxic substances such as algal toxins produced by certain species (such as *Microcystis aeruginosa*) pose an additional threat to aquatic ecosystems and public health [3,4]. The current algae treatment technology faces obvious limitations: chemical methods relying on reagents such as hydrogen peroxide and copper sulfate may cause algal toxin release and secondary pollution [5]; physical methods generally have problems of high energy consumption and membrane pollution [6]; and biological methods carry ecological risks due to introducing exogenous microorganisms. These factors limit the environmental friendliness and sustainability of existing technologies, together.

Check for updates

Academic Editor: Domenico Licursi

Received: 4 December 2025
Revised: 13 January 2026
Accepted: 19 January 2026
Published: 10 February 2026

Copyright: © 2026 by the authors. Licensee MDPI, Basel, Switzerland. This article is an open access article distributed under the terms and conditions of the Creative Commons Attribution (CC BY) license.

Therefore, finding a technical way to realize the harmless treatment of microalgal solid waste and efficient recovery of internal resources at the same time has become a cutting-edge hotspot in the intersection of environmental science and waste management. In terms of the utilization of microalgae resources, the current research mainly focuses on specific conversion pathways, such as anaerobic digestion for biogas production, transesterification for biodiesel, and the extraction of high-value compounds, including β-carotene, phycocyanin, and polyunsaturated fatty acids (PUFAs) [7]. Although these methods have certain technical feasibility, they usually face challenges such as complex process, high energy consumption, or potential environmental risks [7,8]. Taking biodiesel as an example, its production process involves high-energy-consuming links such as dehydration of algae cells, cell wall destruction, esterification reaction, etc. The overall energy output and market competitiveness need to be improved. Simultaneously, in this process, the comprehensive use of ingredients such as protein and carbohydrates is often ignored [9]. In fact, microalgal cells are rich in nutrients available to plants, such as proteins and polysaccharides, which have the potential to directly or indirectly promote plant growth and enhance resistance [10,11]. Against this background, it is a key challenge to realize the utilization of high-value resources by efficiently and selectively recovering and concentrating core bioactive ingredients from the biomass of microalgae, while systematically verifying their agricultural efficacy.

In recent years, a new kind of biopolymers called alginate-like exopolymers (ALEs) has shown considerable prospects in resource recycling application. This is due to their structural and functional characteristics being very similar to those of commercially sodium alginate (SA). Unlike SA, which can be commercially extracted from brown algae, ALEs can be efficiently extracted from aerobic granular sludge, a byproduct of wastewater treatment. Its commercial product "Kaumera" has shown application potential in sectors such as forestry and construction (https://kaumera.com). As the major component of extracellular polymers (EPSs), ALEs are rich in bioactive constituents such as proteins and polysaccharides [12], potentially serving as a biostimulant or soil conditioner. However, current agricultural application research remains almost exclusively focused on sludge systems: while sludge EPSs have demonstrated plant-promoting potential [13,14], their liquid form poses practical challenges for storage and transportation. Further extraction of sludge-derived ALEs improves physical properties but still fails to fully mitigate residual risks from contaminants like heavy metals in the sludge. Therefore, exploring cleaner and more controllable sources of ALEs is crucial for advancing their agricultural applications.

Given the lack of research on the agricultural applications of microalgal-derived ALEs and their advantages of widespread distribution and controllable cultivation, this study selected *C. pyrenoidosa* and *M. aeruginosa*, two widely distributed microalgae in eutrophic water bodies, aiming to preliminarily evaluate the structural composition of microalgal-derived ALEs and their potential correlation with plant growth. The ALEs from both microalgae were first extracted using a Na_2CO_3 extraction–acid precipitation method under heating conditions, with its yield and basic chemical composition evaluated. Subsequently, Fourier transform infrared spectroscopy (FT-IR), ultraviolet–visible spectroscopy (UV–Vis), and three-dimensional electron emission microscopy (3D-EEM) were employed to elucidate their functional group composition, chromophore characteristics, and fluorescent component structures at the molecular level, thereby revealing their potential material basis as plant growth promoters. Finally, through pot experiments with ryegrass, we evaluate the promoting effects and concentration influences of different concentrations of microalgal source ALEs on the growth characteristics and related physiological indicators (e.g., chlorophyll, soluble protein, and polysaccharide) of ryegrass.

2. Materials and Methods

2.1. Experimental Materials

2.1.1. Microalgae Sources and Cultivation

C. pyrenoidosa and *M. aeruginosa* were obtained from the Freshwater Algae Species Bank of the Institute of Aquatic Biology, Chinese Academy of Sciences, Wuhan, Hubei Province, China. To achieve ALE yields comparable to natural blooms, the experiment first expanded algal cells to maximum density. These species were cultured in modified Basal medium (supplemented with 0.5 g/L glucose as carbon source) and modified BG-11 medium (supplemented with 0.3 g/L glucose as carbon source) at 25 °C, under a light intensity of 3000 lx, and a light: dark cycle of 12 h:12 h [15]. The maximum algal cell density during the stationary phase was measured using a hemocytometer, yielding values of 83.1×10^6 cells · mL^{-1} for *C. pyrenoidosa* and 138.1×10^6 cells · mL^{-1} for *M. aeruginosa*. All measurements were repeated 3 times.

2.1.2. Extraction of Alginate-like Exopolymers

Volatile suspended solids (VSSs) were measured using the standard method as shown in Equation (1). Quantitative filter paper was dried in a 105 °C oven (DHG-9140A, Shanghai Yiheng Scientific Instruments, Shanghai, China) to constant weight, weighed, and recorded as m_0. We took 5 g of microalgae (recorded as m), added deionized water (DI water), centrifuged, filtered the precipitate onto filter paper, dried to constant weight to obtain m_1, and dried the crucible to constant weight to obtain m_2. Then, we placed the filter paper and precipitate into the crucible and incinerated it in a muffle furnace (KT-E30, Xiamen Kelie Precision Instruments Co., Ltd., Xiamen, China) at 600 °C for 60 min. After that, it was cooled and weighed to obtain m_3. All measurements were repeated 3 times.

$$\mathrm{VSS} = \frac{m_1 + m_2 - m_3}{m} \quad (1)$$

Referring to the ALE extraction process [16] with appropriate modifications, *C. pyrenoidosa* and *M. aeruginosa* were centrifuged at 4 °C and 4000 r/min for 20 min, and then we collected the pellets and resuspended them. Then, we mixed the pellets with deionized water (DI water) to maintain the ratio of algal suspension and DI water ratio of 6 g: 100 mL. Then, we added 0.5% (*w*/*v*) Na_2CO_3 (Sinopharm Chemical Reagent Co., Ltd., Shanghai, China). The mixture was stirred in a water bath at 80 °C for 30 min to disrupt cell structures and elute ALEs. The mixture was centrifuged at 4 °C and 4000 r/min for 20 min, and the supernatant was collected. We dialyzed the supernatant for 24 h using a dialysis bag with a molecular weight cut-off of 8000–14,000 Da to remove small-molecule impurities. After dialysis, we adjusted the pH of the dialysate to 2.2 ± 0.05 using 1 mol/L HCl (China National Chemical Reagent Co., Ltd., Shanghai, China) to precipitate ALEs. The precipitate was collected by centrifugation again. The pH of the precipitate was adjusted to 8.5 using 0.5 mol/L NaOH (China National Pharmaceutical Group Chemical Reagent Co., Ltd., Shanghai, China) to redissolve and stabilize ALEs. The solution was then diluted to 100 mL with deionized water, and, finally, freeze-dried for 24 h to obtain solid ALEs.

2.1.3. Characterization of Alginate-like Exopolymers

Ultraviolet–visible (UV–Vis) absorbance measurements were performed using a spectrophotometer (DR 5000, HACH, Loveland, CO, USA). Samples were prepared in 2 g/L DI water and analyzed in 1.0 cm quartz cuvettes after instrument calibration with potassium dichromate standard solution. Absorbance spectra were collected over the 200–800 nm range at 1.0 nm resolution, with baseline correction via DI water blank subtraction. Subsequently, key parameters for dissolved organic matter characterization, including the

absorbance ratios E_2/E_3 (A_{250}/A_{365}) and E_4/E_6 (A_{465}/A_{665}), as well as the specific ultraviolet absorbance at 254 nm ($SUVA_{254}$) and 260 nm ($SUVA_{260}$), were calculated according to Equation (2).

$$SUVA_{\lambda} = \frac{A_{\lambda}}{C_{DOC}} \times L \times 100 \quad (2)$$

where A_{λ} represents the corrected absorbance at wavelength λ (254 nm or 260 nm). C_{DOC} represents dissolved organic carbon concentration (mg/L), and L indicates optical path length (1.0 cm). Data processing and visualization were conducted in Origin 2021.

The major functional groups in microalgae-derived ALEs were identified by FT-IR (Nicolet IS50, Thermo Scientific, Waltham, MA, USA). First, 2 mg of freeze-dried ALE powder were mixed with 98 mg of KBr, then ground and pressed into a pellet. Spectra were scanned in the wavenumber range of 400–4000 cm^{-1} at a resolution of 4 cm^{-1}. Spectral data were acquired and processed using OMNIC 9.2 software and exported to Origin 2021 for plotting. Prior to testing, baseline correction was performed by subtracting the background spectrum of pure KBr pellets to eliminate matrix interference.

Fluorescent compounds in ALEs were identified using 3D excitation-emission matrix (EEM) fluorescence spectroscopy (Fluoro Max-4, Horiba, Kyoto, Japan). ALE samples were diluted to 2 g/L with DI water and measured in 1.0 cm quartz cuvettes. Spectra were acquired with excitation (E_x) 200–500 nm, emission (E_m) 220–550 nm, scan rate 1200 nm/min, and slit width 5 nm, following quinine sulfate calibration and blank subtraction. Fluorescence peaks were qualitatively identified against a standard database. The EEM spectrum was divided into five characteristic regions [16,17] for integral calculation. Data visualization was performed using Origin 2021.

2.1.4. Model Plants and Culture Substrates

Lolium perenne L. (hereinafter referred to as ryegrass), obtained from Lvguan Grass Industry Co., Ltd., Beijing, China, was chosen as the model plant. The cultivation substrate comprised native sand sourced from the Tengger Desert (37.6425° N, 103.1675° E), which represents a typical northwest sandy degraded substrate in northwestern China. Prior to use, the sand was passed through a 20-mesh sieve to eliminate gravel.

2.2. Microalgae-Derived Fertilizer Cultivation Experiment

2.2.1. Experimental Design

Four microalgae-derived fertilizers were used: *C. pyrenoidosa* whole-cell fertilizer (Cp-CF), *C. pyrenoidosa* ALE fertilizer (Cp-ALE), *M. aeruginosa* whole-cell fertilizer (Ma-CF), and *M. aeruginosa* ALE fertilizer (Ma-ALE). The fertilizers were applied at dry weight ratios to the sandy substrate of 1:10,000, 1:5000, and 1:2000, with a control group (no fertilizer). The centrifuged algal pellets and freeze-dried ALEs were each dissolved in 100 mL DI water and mixed into a sandy substrate. Ryegrass was planted in the prepared substrates (initial nutrient contents in Table 1) under controlled conditions: light intensity (300–350 $\mu mol \cdot m^{-2} \cdot s^{-1}$), monitored using an illuminance meter (ST-85, Beijing Normal University Photoelectric Technology Co., Ltd., Beijing, China) with a 21 ± 4 °C day/16 ± 2 °C night, and 45–60% relative humidity. Daily watering was maintained at 20 mL, and each treatment was replicated 3 times for 30 d.

2.2.2. Determination of Plant Physicochemical Indicators

Growth characteristics: 30 days after planting, five plants were randomly selected from each pot, and the plant height and root length were determined by straightedge (accuracy 0.1 cm); the fresh weight was determined by electronic balance (BSA224S, Sartorius Group, Göttingen, Germany); and the dry weight was determined by killing in an oven at 105 °C

(DHG-9140A, Shanghai YIHEONG Scientific Instrument, Shanghai, China) for 30 min and drying at 75 °C until constant weight.

Table 1. Initial nutrient composition of sandy planting substrate in different treatment groups.

Fertilizer	Treatment	Available Nitrogen (mg/kg)	Available Phosphorus (mg/kg)	Available Potassium (mg/kg)
Cp-CF	Control	13.75 ± 0.08	2.37 ± 0.04	52.67 ± 1.28
	1:10,000	179.36 ± 1.23	41.37 ± 0.48	197.31 ± 2.17
	1:5000	271.93 ± 0.53	52.91 ± 0.23	210.45 ± 1.17
	1:2000	259.37 ± 1.14	68.39 ± 0.73	263.72 ± 2.03
Cp-ALE	1:10,000	159.21 ± 1.17	32.41 ± 0.27	176.72 ± 0.41
	1:5000	93.43 ± 1.27	41.73 ± 1.05	229.85 ± 2.23
	1:2000	236.84 ± 2.11	52.03 ± 0.93	230.45 ± 2.37
Ma-CF	Control	13.75 ± 0.08	2.37 ± 0.04	52.67 ± 1.28
	1:10,000	104.68 ± 2.07	23.47 ± 0.43	134.72 ± 3.12
	1:5000	167.38 ± 1.37	34.57 ± 1.02	184.85 ± 1.72
	1:2000	204.68 ± 2.07	56.38 ± 1.27	237.68 ± 2.13
Ma-ALE	1:10,000	97.41 ± 0.34	19.54 ± 0.12	126.82 ± 1.23
	1:5000	127.98 ± 1.37	36.77 ± 0.73	175.64 ± 0.97
	1:2000	176.51 ± 1.45	51.92 ± 0.81	213.25 ± 1.08

Main nutrients: soluble protein (PN) content was determined by the Lorry method, the reagent was purchased from Shanghai Sangong (No. C504021), the absorbance was measured at 500 nm by an ultraviolet spectrophotometer (N4S, Shanghai Yidian, Shanghai, China), and bovine serum albumin was used as a standard; polysaccharide (PS) content was determined by the phenol-sulfuric acid method, 5% phenol was mixed with 98% concentrated sulfuric acid at a rate of 1:5, and absorbance was measured at 490 nm. The polysaccharide (PS) content was determined by the phenol-sulfuric acid method, 5% phenol mixed with 98% concentrated sulfuric acid at 1:5, the absorbance was measured at 490 nm, and glucose was used as the standard; the chlorophyll content was determined by the ethanol extraction method, 0.1 g of fresh leaves was extracted with 80% ethanol and kept away from the light for 24 h, and the absorbance was measured at 663 and 645 nm; and the chlorophylls a and b and the total chlorophyll content were calculated by Arnon formula. The data were organized using Excel 2021; one-way analysis of variance (ANOVA) was performed using SPSS 26.0 and the significance of the differences was tested using Duncan's multiple comparisons ($p < 0.05$), and the graphs were plotted using Origin 2021.

3. Results and Discussion

3.1. ALE Components and Spectral Characteristics

3.1.1. ALE Component Properties Analysis

Component analysis revealed that both microalgal-derived ALEs possess a distinct material basis for functioning as biofertilizers (Table 2). Studies have confirmed that the composition and proportion of ALE components are the key factors that determine its functional characteristics [18]. Among them, protein (PN) and polysaccharide (PS) are important nutrient precursors and signal molecules necessary for plant growth, and their content is directly related to the promoting effect of ALEs on plants. This study found that PN is the core functional component in both ALEs, among which the PN and PS content of Cp-ALE is significantly higher than that of Ma-ALE. This is of great significance: as a natural biological stimulant, protein hydrolysates play a crucial role

in inducing defensive compounds (such as peptides, amino acids, and hormones) in plants [19]; polysaccharides in the fertilizer might improve substrate water retention [20], which supports sustained nutrient availability for plants. The synergy between these two components constitutes the core mechanism of ALE's growth function.

Table 2. Yield and composition of ALEs from different sources.

Source	Productivity/(mg·g^{-1} VSS)	PN/(mg·g^{-1})	PS/(mg·g^{-1})	PN/PS
Chlorella pyrenoidosa	35.34 ± 4.32	213.20 ± 13.12	53.41 ± 2.11	4.02
Microcystis aeruginosa	24.89 ± 1.23	140.21 ± 7.21	32.93 ± 3.62	4.26

On this basis, this study uses the PN/PS ratio to further evaluate their fertilizer potential. The PN/PS values of Cp-ALE and Ma-ALE are 4.02 and 4.26, respectively, the extracellular protein components (especially Ma-ALE) are richer, and the best balance of "promoting activity–structural stability" is achieved. This provides strong evidence of their efficacy as a high-performance plant growth promoter. The yield of Cp-ALE is significantly higher than that of Ma-ALE, indicating that *C. pyrenoidosa* has a greater advantage in ALE enrichment and high-value fertilization. These compositional characteristics lay a solid foundation for subsequent molecular structure analysis.

3.1.2. Ultraviolet–Visible Spectroscopy (UV–Vis) Analysis

UV–Vis spectroscopy analysis provides molecular-level evidence for the fertilizer functional properties of ALEs (Figure 1). The results show that strong absorption at 200–210 nm indicates the presence of carboxyl or ester functional groups in ALEs, which helps to enhance their binding ability with soil nutrients [21,22], which are theoretically associated with metal-binding and nutrient interaction capacities. Absorption peaks in the range of 240–290 nm suggest the presence of aromatic proteins and humic-acid-like components.

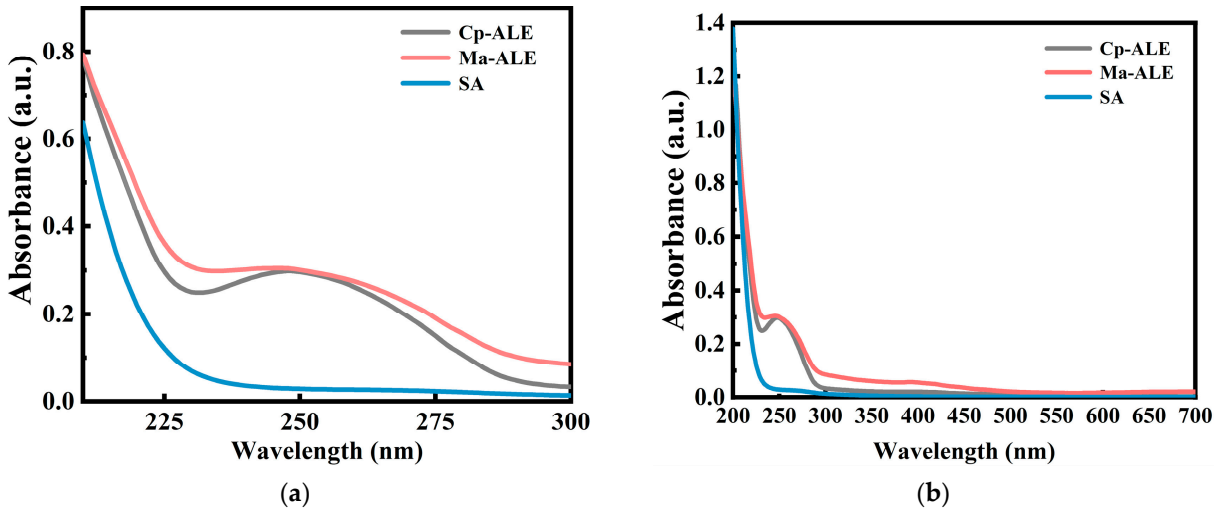


Figure 1. UV–Vis spectra of microalgae ALE: (**a**) 210–300 nm range; (**b**) 200–700 nm range.

Further spectral index analysis [23] (Table 3) revealed that Ma-ALE exhibited significantly lower E_2/E_3, E_4/E_6, and E_2/E_4 values compared to Cp-ALE, indicating a higher proportion of aromatic components and greater molecular weight in its structure. Conversely, the spectral profile of Cp-ALE suggests a more aliphatic character, which could be linked to higher biodegradability.

Table 3. UV–Vis spectral indices of ALE derived from microalgae.

Index	$SUVA_{254}$	$SUVA_{260}$	E_2/E_3	E_4/E_6	E_2/E_4
Cp-ALE	0.77	0.70	14.62	3.02	15.06
Ma-ALE	1.31	1.23	5.33	1.49	6.23

Based on these structural distinctions and supported by previous studies on similar substances, we hypothesize that Ma-ALE and Cp-ALE may exhibit divergent behaviors in agricultural settings. These structural differences suggest distinct functional properties for agricultural applications. Ma-ALE's high aromaticity and molecular weight may enhance its persistence in soil, while Cp-ALE's greater aliphatic nature could promote rapid nutrient release. This result conducted a preliminary exploration of the potential of microalgae-derived ALEs as fertilizers and initially clarified their structural basis, providing a basis for subsequent in-depth characterization and practical application verification.

3.1.3. Fourier Transform Infrared (FT-IR) Spectroscopy Analysis

FT-IR spectral analysis revealed the growth-promoting potential of microalgal-derived ALE at the molecular level. Figure 2 shows the characteristic absorption peaks of key wave numbers closely related to the nutritional function of ALEs derived from two microalgae: 1657 cm^{-1} (protein amide I band, C=O stretching vibration) and 1535 cm^{-1} (protein amide II band, N–H bending/C–N stretching), confirming that there are protein components in ALEs that are easily absorbed by plants. The absorption peak near 1074 cm^{-1} corresponds to the C–O–C/C–N bond vibrations of the polysaccharides, indicating that the polysaccharide has the effect of plant biostimulant.

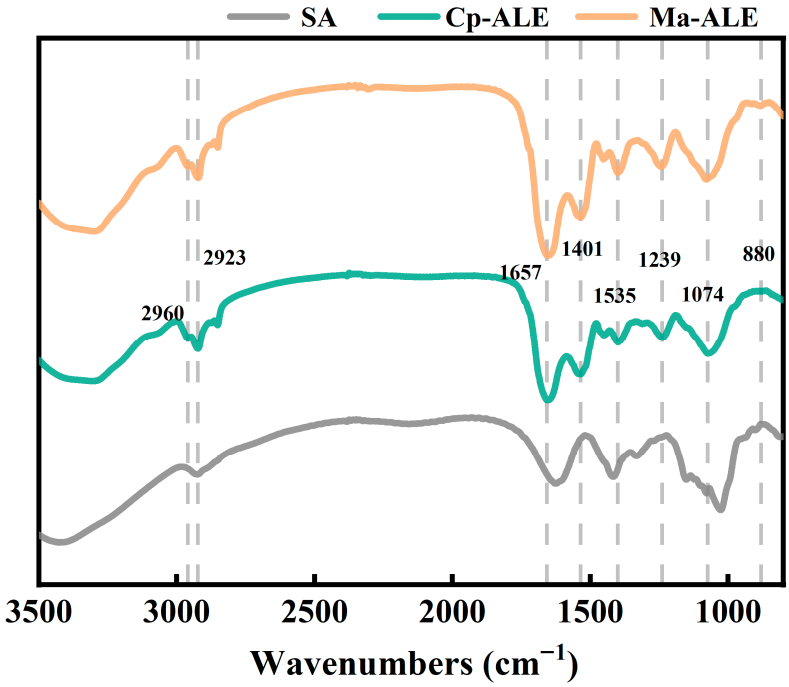


Figure 2. FT-IR spectra of ALEs from different sources (SA: commercially available alginate; Cp-ALE: *Chlorella pyrenoidosa* ALE; Ma-ALE: *Microcystis aeruginosa* ALE).

The above spectral characteristics jointly confirm that microalgae-sourced ALE is a functional organic mixture composed of proteins, polysaccharides, and other components, and its biomolecular composition is similar to that of ALEs extracted from previously reported active sludge [24,25]. In terms of growth-promoting mechanism, active amino acids released through protein water interpretation may play a direct role in regulating

the synthesis of plant hormones [26]; polysaccharides indirectly improve the efficiency of nutrient absorption by improving the inter-root microenvironment (such as optimizing soil structure and regulating microbial communities). This synergy provides important structural evidence for the agricultural application of microalgae-derived ALEs.

3.1.4. Three-Dimensional Fluorescence Spectroscopy (3D-EEM) Analysis

We used 3D-EEM technology to evaluate the fertilizer potential of ALEs derived from microalgae, with the results shown in Figure 3. I denotes aromatic protein I, II denotes aromatic protein II, III denotes furan-containing compounds, IV denotes soluble microbial products, and V denotes humic compounds. Both ALEs showed characteristic fluorescence peaks in protein-like fluorescence regions. Preliminary analysis based on peak distribution patterns indicates that Peak A in Region II may belong to tryptophan-containing proteins, which have been confirmed as precursors for auxin synthesis [27], potentially directly promoting plant root development and cell division. Peak B in region IV is presumed to be associated with soluble microbial metabolites (e.g., proteinaceous substances rich in tryptophan and tyrosine). These substances may enhance plant stress resistance by participating in the synthesis pathways of key photosystem enzymes while regulating plant growth [28].

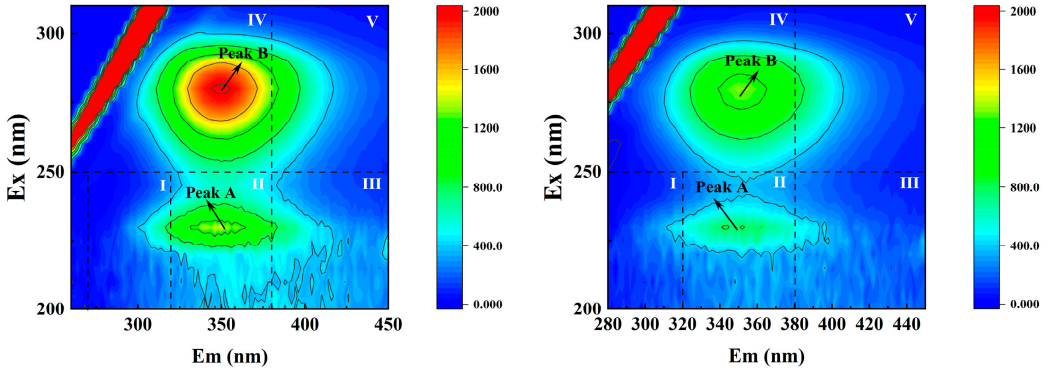


Figure 3. Fluorescence component identification in ALEs from different sources by 3D-EEM: (**a**) Cp-ALE; (**b**) Ma-ALE.

It is noteworthy that the fluorescence intensity of Cp-ALE in Region IV is significantly higher than in Ma-ALE. This result provides preliminary molecular evidence for the fertilizer potential of Cp-ALE and lays the foundation for systematic evaluation of the fertilizer value of ALEs from different microalgal species.

3.2. Regulatory Effect and Mechanism of Microalgae-Derived Fertilizers on Ryegrass

3.2.1. Effect of Microalgae-Derived Fertilizers on Growth Characteristics of Ryegrass

The effects of four microalgae-derived fertilizers (Cp-CF, Cp-ALE, Ma-CF, Ma-ALE) on ryegrass biomass exhibited a significant "low-promoting and high-suppressing" effect, as shown in Figure 4 and Table 4. This phenomenon aligns with the concentration response patterns of microalgae fertilizers in plant growth regulation [10,29]. At the optimal concentration of 1:10,000, dry weight in all treatment groups significantly exceeded that of the control group. Specifically, Cp-CF and Cp-ALE increased dry weight by 64.4% and 61.2%, respectively, while Ma-CF and Ma-ALE increased it by 64.3% and 59.8%.

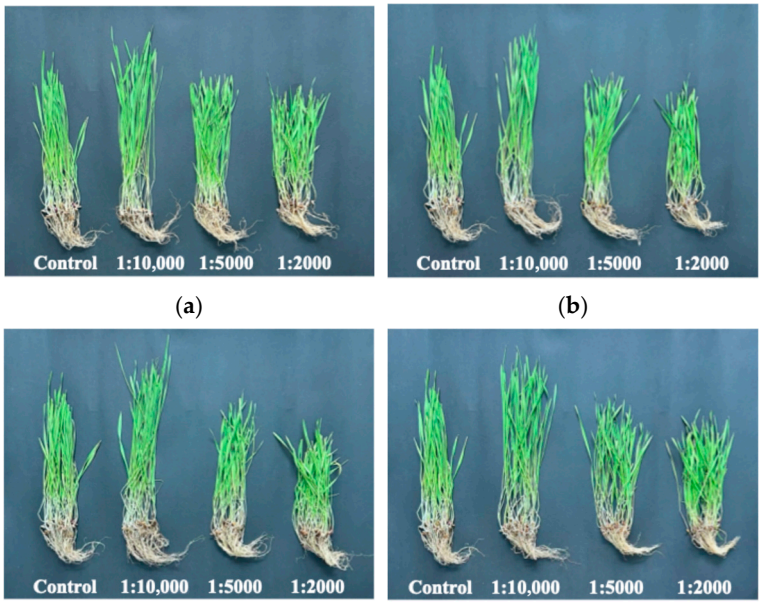


Figure 4. Harvest phenotypes of ryegrass under different concentrations of microalgae-derived fertilizer treatments: (**a**) Cp-CF; (**b**) Cp-ALE; (**c**) Ma-CF; (**d**) Ma-ALE.

Table 4. Effects of different sources of derived fertilizers on growth characteristics of ryegrass.

Fertilizer	Treatment	Plant Height (cm)	Root Length (cm)	Fresh Weight (g)	Dry Weight (g)
Cp-CF	Control	16.80 ± 0.14 c	17.56 ± 0.47 bc	0.98 ± 0.02 c	0.13 ± 0.01 b
	1:10,000	20.54 ± 0.66 a	20.35 ± 1.20 a	1.33 ± 0.15 a	0.21 ± 0.01 a
	1:5000	18.71 ± 0.71 b	17.94 ± 1.34 b	1.17 ± 0.05 ab	0.13 ± 0.01 b
	1:2000	14.86 ± 0.48 d	15.44 ± 0.16 e	0.85 ± 0.02 cd	0.08 ± 0.01 e
Cp-ALE	1:10,000	20.65 ± 0.49 a	21.25 ± 1.06 a	1.36 ± 0.06 a	0.22 ± 0.02 a
	1:5000	17.72 ± 0.71 bc	15.90 ± 0.1 cd	1.01 ± 0.14 bc	0.11 ± 0.01 d
	1:2000	15.21 ± 0.64 d	15.06 ± 0.23 e	0.79 ± 0.008 d	0.08 ± 0.01 e
Ma-CF	Control	16.80 ± 0.14 b	17.56 ± 0.47 b	0.98 ± 0.02 b	0.13 ± 0.01 b
	1:10,000	21.21 ± 2.82 a	22.60 ± 0.67 a	1.21 ± 0.02 a	0.21 ± 0.01 a
	1:5000	15.04 ± 0.67 bc	15.12 ± 0.12 b	0.90 ± 0.05 bc	0.11 ± 0.01 c
	1:2000	13.06 ± 1.33 c	11.62 ± 0.59 d	0.71 ± 0.03 d	0.06 ± 0.01 d
Ma-ALE	1:10,000	20.65 ± 0.92 a	21.65 ± 2.23 a	1.36 ± 0.09 a	0.19 ± 0.02 a
	1:5000	15.41 ± 0.72 bc	14.51 ± 0.53 b	0.89 ± 0.04 c	0.10 ± 0.01 c
	1:2000	13.22 ± 1.41 c	11.94 ± 0.08 d	0.71 ± 0.02 d	0.06 ± 0.003 d

Note: Different lower case letters after the data in the same column indicate significant differences between treatment concentrations of the same algal species ($p < 0.05$, Duncan's multiple comparison).

This growth-promoting effect shows a potential correlation with prior component analysis results: 3D-EEM revealed higher fluorescence intensity corresponding to tryptophan-derived components (Peak B) in Cp-ALE. These components may serve as precursors for indole-3-acetic acid (IAA) synthesis, potentially promoting auxin production, thereby enhancing plant cell division and biomass accumulation. Meanwhile, in the UV–Vis spectrum, the high ratio of E_2/E_3 and E_4/E_6 suggests that ALEs may indirectly promote plant growth by relatively enriching degradable polysaccharides to improve the rhizosphere microenvironment and enhance nutrient absorption efficiency [30].

It is worth noting that there is no significant difference in the growth promotion effect of ALE fertilizer and CF under the same algae source at all concentrations ($p > 0.05$). At the best concentration of 1:10,000, the dry weight increase in Cp-ALE (61.2%) is close to that of Cp-CF (64.4%), and the dry weight increase in Ma-ALE (59.8%) is comparable to that of Ma-CF (64.3%). These results indicate that ALEs obtained through the simple extraction process employed can achieve growth-promoting effects comparable to CF for ryegrass, providing a feasible foundation for the efficient utilization and high-value conversion of microalgal biomass.

When the fertilizer concentration was increased to 1:2000, all treatment groups inhibited ryegrass growth. The *M. aeruginosa* group exhibited stronger inhibition, with dry weight inhibition rates of 52.3–54.7% and root length inhibition rates of 31.2–33.8%. The *C. pyrenoidosa* group showed weaker inhibition, with corresponding inhibition rates of 38.5–40.1% and 12.07–14.23%. This inhibitory effect may be related to osmotic stress caused by elevated levels of readily available nitrogen, phosphorus, and potassium resulting from high-concentration fertilization. Furthermore, the inhibition effect in the *M. aeruginosa* group was significantly stronger than in the *C. pyrenoidosa* group. This difference may be associated with the microcystin-LR (MC-LR) potentially produced by *M. aeruginosa* to plant roots [31].

3.2.2. Effect of Microalgae-Derived Fertilizer on Physiological Indices of Ryegrass

The concentrations of chlorophyll, soluble protein, and soluble polysaccharides serve as crucial physiological indicators of plants' photosynthetic capacity, nitrogen metabolism intensity, and carbon storage status. This study found that microalgae-derived fertilizers significantly enhanced soluble protein content while promoting chlorophyll accumulation, with this effect exhibiting a marked concentration dependence (Figures 5 and 6). However, no significant impact was observed on the content of soluble polysaccharides. These findings suggest that microalgae-derived fertilizers may exert their effects by preferentially regulating nitrogen assimilation and photosynthetic apparatus development rather than the conversion of carbon skeletons into polysaccharides, demonstrating their potential for selective modulation of plant metabolic pathways.

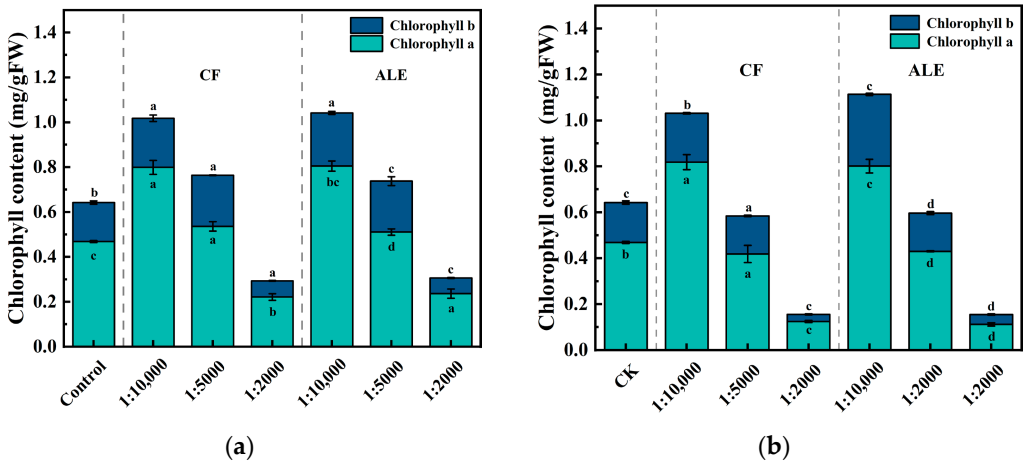


Figure 5. Effect of microalgae-derived fertilizer on chlorophyll content in ryegrass: (**a**) *Chlorella pyrenoidosa*; (**b**) *Microcystis aeruginosa*. Note: Different lower case letters after the data in the same column indicate significant differences between treatment concentrations of the same algal species ($p < 0.05$, Duncan's multiple comparison).

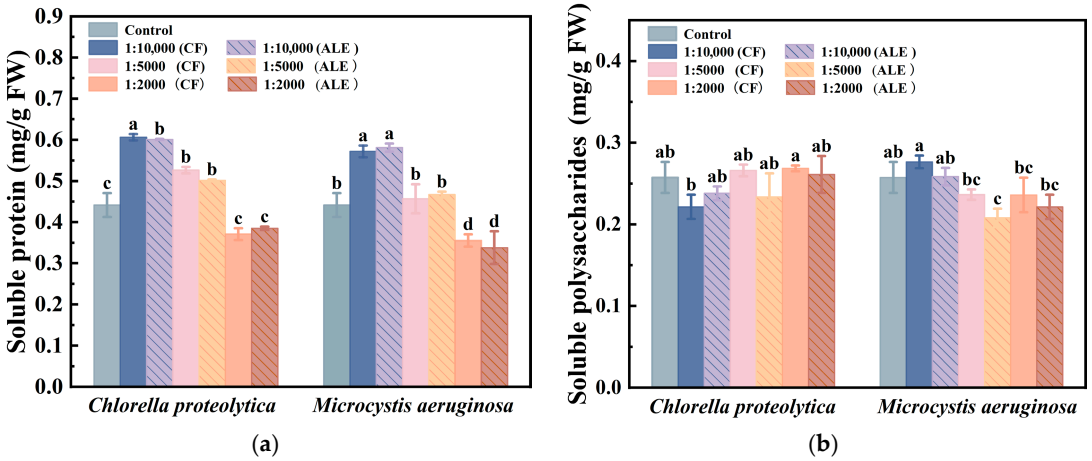


Figure 6. Effects of microalgae-derived fertilizers on the synthesis in ryegrass: (**a**) soluble proteins; (**b**) soluble polysaccharides. Note: Different lower case letters after the data in the same column indicate significant differences between treatment concentrations of the same algal species ($p < 0.05$, Duncan's multiple comparison).

In terms of chlorophyll synthesis, when the optimal concentration was 1:10,000, all treatments significantly increased the chlorophyll content ($p < 0.05$), among which the effect of CF and ALE treatment was comparable: the chlorophyll a, b, and total chlorophyll content of the Cp-CF and Cp-ALE groups increased by 70.5%, 25.9%, and 67.3%, respectively, compared with the control, while the Ma-CF and Ma-ALE groups showed a consistent and significant upward trend. This result aligns with Gao et al.'s [32] observation that "microalgal fertilizers can influence plant chlorophyll synthesis". It is hypothesized that such microalgal-derived ALEs may enhance photosynthetic efficiency by increasing chlorophyll (chlorophyll a and b) content, thereby helping to maintain or elevate photosynthetic activity.

However, when the concentration was increased to 1:2000, both microalgal-derived fertilizers strongly inhibited chlorophyll a and b, and the inhibition of chlorophyll b was more obvious. Among them, the decrease in chlorophyll a in the Ma-ALE treatment group (71.5%) was significantly greater than that in the Cp-ALE treatment group (50.3%), and the decrease in chlorophyll b reached 82.1%, which was significantly higher than that in the Cp-ALE treatment group (57.9%). This difference may be related to the complex composition of Ma-ALE. UV–Vis spectral analysis shows that its extract contains a certain amount of aromatic substances, but the relationship between such substances and chlorophyll synthesis inhibition is not clear. It is worth noting that the reduction in chlorophyl b in this study is significantly higher than that of chlorophyl a, which is consistent with the existing research conclusions that chlorophyl b is more sensitive to abiotic coercion as the main pigment of the light capture complex (LHC) [33].

At a concentration of 1:10,000, Cp-ALE treatment significantly increased soluble protein content by 35.2% compared to the control group, exceeding the increase observed in the Ma-ALE treatment group (27.8%). FT-IR spectral analysis revealed characteristic absorption peaks at 1657 cm^{-1} (amide I band, C=O stretching vibration) and 1535 cm^{-1} (amide II band, N-H bending vibration), indicating the presence of protein components in both ALEs. Furthermore, the Cp-ALE group exhibited higher E_2/E_3 and E_4/E_6 ratios, suggesting that its protein structure may be more readily absorbed by roots or degraded into small molecule amino acids, thereby demonstrating greater potential for promoting nitrogen assimilation and protein accumulation. When the concentration increased to 1:2000, soluble protein content significantly decreased in all treatment groups, with reductions of 18.2% in the *M. aeruginosa* group and 19.5% in the *C. pyrenoidosa* group. This decline aligns

with classical theories suggesting that excess nitrogen sources disrupt carbon–nitrogen balance, thereby inhibiting protein synthesis [34].

The FT-IR spectrum detected the characteristic absorption peak of the polysaccharide component in the microalgae-derived ALE at 1074 cm^{-1} (corresponding to the C-O-C stretching vibration), indicating that it contains polysaccharide substances. However, after the application of microalgae-derived fertilizer, there was no significant difference in the content of soluble polysaccharides in ryegrass between each treatment group and the control group ($p < 0.05$). This indicates that the promoting effect of microalgae-derived fertilizers on plant growth in this study is more likely to be related to nitrogen metabolism, including providing nitrogen sources and protein synthesis precursors, while the impact on carbohydrate synthesis and accumulation is relatively limited.

3.3. Economic Benefits

Current mainstream microalgal biorefinery pathways, including the production of biodiesel and the extraction of high-value products such as β-carotene, phycocyanin, astaxanthin, and polyunsaturated fatty acids (PUFAs), still face numerous practical challenges, including process complexity, high energy consumption, and significant environmental risks. These processes typically involve multiple steps, including cell destruction, solvent extraction, esterification, and multi-stage purification, requiring the use of various organic solvents such as methanol, ethyl acetate, and petroleum ether, along with corresponding catalysts. These operations generate alcohol-containing wastewater and organic residues with high chemical oxygen demand (COD) and salinity, posing potential threat to the ecological environment. From an economic perspective, although the market price of some algae pigments is very high (USD 46.5–3608.5/kg) [35–37], the price of microalgae-derived biodiesel is still relatively low, at about USD 1.9–2.2/L [38]. Coupled with the high process treatment costs and additional economic pressures from subsequent pollutant disposal, the overall economic viability and environmental sustainability of such microalgal refining pathways face significant challenges.

In contrast, extracting ALEs from microalgae has significant comprehensive advantages. The method is mainly based on acid coagulation, which simplifies the process and only requires conventional acid and alkali reagents, avoiding the use of most toxic organic solvents and, thus, reducing environmental risks and processing costs from the source. Moreover, the intermediate product EPSs extracted in this process have considerable potential for resource recovery [39–42]. The final ALE product is obtained in solid form, which greatly improves the convenience of storage and transportation and provides favorable conditions for large-scale agricultural applications.

Furthermore, the feasibility of this technology has been proven in the pilot project of Zutphen and Epet in the Netherlands. The ALE product "Kaumera" comes from sludge, and the price is about USD 2.20/kg (https://www.aquatechtrade.com). Considering the comparable moisture content of microalgae and sludge, as well as the uniformity of extraction reagents and processes, we have reason to infer that ALEs from microalgae have similar market competitiveness, and the preliminary estimate is very close to Kaumera's results.

4. Conclusions

This study proposed a resource utilization method for ALE extraction of algae waste using *C. pyrenoidosa* and *M. aeruginosa*. The results show that the two sources of ALEs mainly contain protein and polysaccharide. Cp-ALE has a high extraction rate (35.34 ± 4.32 $mg \cdot g^{-1}$ VSS) rich levels of protein, polysaccharides, and tryptophan. In the ryegrass experiments, all algae-derived fertilizers showed the effect of "low concentration promotion and high concentration inhibition". At a concentration of 1:10,000, the

dry matter quality of rye grass increased by 64.4%. There is no significant difference in the effect of ALE fertilizer and CF fertilizer of the same species, indicating that microalgae effectively retain growth-promoting biomass. Its mechanism involves regulating nitrogen metabolism and increasing the content of chlorophyll a and soluble protein. However, at high concentrations (1:2000), all fertilizers inhibited growth, and the *M. aeruginosa* group showed stronger inhibition, which may be due to algae toxins (MC-LR). Nevertheless, this method offers a novel approach for the resource recovery of algal waste, providing both environmental and economic benefits. Given the potential risks at high concentrations, the field applicability of Ma-ALE and the environmental fate of its toxins require further evaluation. Future research should focus on root microbiome regulation, field application validation, nutrient dynamics, and long-term safety. Concurrently, parallel factor analysis (PARAFAC) should be adopted to conduct precise qualitative and quantitative analysis of the key components of ALEs to clarify their potential mechanisms.

Author Contributions: Conceptualization, methodology, investigation, formal analysis, writing—original draft preparation, Y.X.; conceptualization, methodology, formal analysis, visualization, F.Y.; data curation, visualization, S.L.; data curation, validation, L.L.; conceptualization, funding acquisition, project administration, supervision, writing—review and editing, X.S. All authors have read and agreed to the published version of the manuscript.

Funding: This study was supported by the High-End Foreign Experts Program of China (grant No. G2023025010L).

Institutional Review Board Statement: Not applicable.

Informed Consent Statement: Not applicable.

Data Availability Statement: Part of the data used in this study was obtained from a previous work by Fan Yi (in press at Journal of Qingdao University of Technology). The data are available from the corresponding author of that study upon reasonable request. The remaining data generated in this study are available from the corresponding author of this article upon request.

Conflicts of Interest: The authors declare no conflicts of interest.

References

1. Xie, Y.X.; Chen, S.R.; Zhou, F.; Wang, J.; Liu, Y.N.; Gao, Y.C.; Yan, X.L.; Deng, K.; Chen, C. Development of a hybrid algal population prediction (HAPP) model by algae growth potential estimation and time series regression and its application in one reservoir in China. *Water Res.* **2025**, *287*, 1244119. [CrossRef] [PubMed]
2. Wang, Y.; Zhao, D.; Woolway, R.I.; Yan, H.R.; Paerl, H.W.; Zheng, Y.; Zheng, C.M.; Feng, L. Global elevation of algal bloom frequency in large lakes over the past two decades. *Natl. Sci. Rev.* **2025**, *12*, 3. [CrossRef]
3. Wang, J.; Cheng, G.F.; Zhang, J.H.; Shangguan, Y.Y.; Lu, M.; Liu, X.G. Feasibility and mechanism of recycling carbon resources from waste cyanobacteria and reducing microcystin toxicity by dielectric barrier discharge plasma. *J. Hazard. Mater.* **2023**, *460*, 132333. [CrossRef]
4. Guo, Z.H.; Hu, J.Q.; Li, J.M.; Xia, X.Y. Unraveling the effects of allelopathic algicide on *Microcystis* population: Microcystin pollution risk assessment and proteomic-metabolomic insights into the sensitivity of toxigenic and non-toxigenic strains. *J. Hazard. Mater.* **2025**, *495*, 138671. [CrossRef]
5. Lürling, M.; Liao, Z.W.; Kang, L.; Bishop, W.M.; Mucci, M. Effects of peroxide-based compounds on growth and toxicity of *Microcystis aeruginosa*. *Harmful Algae* **2025**, *149*, 102930. [CrossRef] [PubMed]
6. Mohamed, A.; Owis, E.; Abdel-Fattah, G.; Eladle, E. Optimising *Chlorella vulgaris* bioflocculation by *Aspergillus Niger* pellets and their application in wastewater treatment and lipid production. *Microb. Cell Fac.* **2025**, *24*, 229. [CrossRef]
7. Saeker, N.K.; Kaparaju, P. Microalgal Bioeconomy: A Green Economy Approach Towards Achieving Sustainable Development Goals. *Sustainability* **2024**, *16*, 11218. [CrossRef]
8. Kumar, M.; Rathour, R.; Singh, R.; Sun, Y.Q.; Pandey, A.; Gnansounou, E.; Lin, K.Y.; Tsang, D.C.; Thakur, I.S. Bacterial polyhydroxyalkanoates: Opportunities, challenges, and prospects. *J. Clean. Prod.* **2020**, *263*, 121500. [CrossRef]

9. Chandrasekhar, K.; Raj, T.; Ramanaiah, S.; Ramanaiah, S.; Kumar, G.; Banu, J.R.; Varjani, S.; Sharma, P.; Pandey, A.; Kumar, S.; et al. Algae biorefinery: A promising approach to promote microalgae industry and waste utilization. *J. Biotechnol.* **2022**, *345*, 1–16. [CrossRef]
10. Cordeiro, E.C.N.; Mógor, Á.F.; Amatussi, J.O.; Mógor, G.; Marques, H.M.; de Lara, G.B. Microalga biofertilizer improves potato growth and yield, stimulating amino acid metabolism. *J. Appl. Phycol.* **2022**, *34*, 385–394. [CrossRef]
11. Khan, S.; Thaher, M.; Abdulquadir, M.; Faisal, M.; Meharlya, S.; Al-Najjar, M.A.A.; Al-Jabri, H.; Das, P. Utilization of Microalgae for Urban Wastewater Treatment and Valorization of Treated Wastewater and Biomass for Biofertilizer Applications. *Sustainability* **2023**, *15*, 16019. [CrossRef]
12. Wang, W.Y.; Zhang, Y.F.; Man, J.M.; Li, X.S.; Li, R.D. Optimal extraction and characterization of alginate-like extracellular polymers (ALE) and proteins from wastewater sludge. *Microchem. J.* **2025**, *210*, 113033. [CrossRef]
13. Bahgat, N.T.; Wilfert, P.; Picken, S.J.; Sorin, L.; Lin, Y.M.; Korving, L.; van Loosdrecht, M.C.M. Impact of phosphorus on the functional properties of extracellular polymeric substances recovered from sludge. *Water Res.* **2025**, *274*, 123019. [CrossRef] [PubMed]
14. Shi, C.; Yuan, S.C.; Zhang, L.; Wang, X.Y.; Hao, L.T.; Su, S.M.; Lei, Z.F.; Hao, X.D. Coating seeds with biopolymers extracted from waste-activated sludge. *Sustain. Chem. Pharm.* **2024**, *39*, 101519. [CrossRef]
15. Zhao, F.C.; Li, Z.X.; Zhou, X.L.; Chu, H.Q.; Jiang, S.H.; Yu, Z.J.; Zhou, X.F.; Zhang, Y.L. The comparison between vibration and aeration on the membrane performance in algae harvesting. *J. Membr. Sci.* **2019**, *592*, 117390. [CrossRef]
16. Felz, S.; Al-Zuhairy, S.; Aarstad, O.A.; van Loosdrecht, M.C.; Lin, Y.M. Extraction of Structural Extracellular Polymeric Substances from Aerobic Granular Sludge. *J. Vis. Exp.* **2016**, *115*, 54534. [CrossRef]
17. Chen, W.; Westerhoff, P.; Leenheer, J.A.; Booksh, K. Fluorescence excitation−emission matrix regional integration to quantify spectra for dissolved organic matter. *Environ. Sci. Technol.* **2003**, *37*, 5701–5710. [CrossRef]
18. Rehman, Z.U.; Ghaani, M.; Mohamed, A.Y.; Gallagher, J.; Salkaiy, P.E.; Ali, M. Alginate-like exopolysaccharides extracted from different waste sludges exhibit varying physicochemical and material properties. *Front. Microbiol.* **2024**, *15*, 1493782. [CrossRef]
19. Munarod, D.; Mazo, C.H.; Bauer, C.M.; da Silva Gomes, L.; Teodoro, E.B.; Mazzarino, L.; da Rocha Veleirinho, M.B.; Moura e Silva, S.; Maraschin, M. A novel biostimulant from chitosan nanoparticles and microalgae-based protein hydrolysate: Improving crop performance in tomato. *Sci. Hortic.* **2024**, *323*, 112491. [CrossRef]
20. Khanams, S.; Yeasmin, F.; Mondal, A.K.; Naim, M.R.; Chowdhury, A.; Ray, S.K. Redox-driven ultrafast synthesis of lignin-based hydrogel: Optimization, characterization and prospects for slow NPK-fertilizer release under varied environmental conditions. *Ind. Crops Prod.* **2025**, *237*, 122199. [CrossRef]
21. Zhu, Y.C.; Zhang, M.; Han, X.Z.; Lu, X.C.; Chen, X.; Feng, H.L.; Wu, Z.M.; Liu, C.Z.; Yan, J.; Zou, W.X. Evaluation of the soil aggregate stability under long term manure and chemical fertilizer applications: Insights from organic carbon and humic acid structure in aggregates. *Agric. Ecosyst. Environ.* **2024**, *376*, 109217. [CrossRef]
22. Cornelis, J.T.; De, T.F. Soil controls on carboxylate-driven processes and opportunities. *Plant Soil* **2022**, *476*, 239–250. [CrossRef]
23. Li, J.; Hao, X.D.; Gam, W.; An Loosdrecht, M.C.M.; Wu, Y.Y. Controlling factors and involved mechanisms on forming alginate like extracellular polymers in flocculent sludge. *Chem. Eng. J.* **2022**, *439*, 135792. [CrossRef]
24. Shi, C.; Zeng, R.G.; Hap, L.T.; Hao, X.D.; Li, J. Extracting compositional blocks of alginate-like extracellular polymers (ALE) from conventional activated sludge (CAS). *Sci. Total Environ.* **2023**, *867*, 161371. [CrossRef] [PubMed]
25. Yang, Y.J.; Zhou, H.; Liu, W.L.; Wang, K.; Yu, T. Effect of extraction temperature on value-added biopolymer recovery in waste activated sludge. *Water Cycle* **2025**, *6*, 272–277. [CrossRef]
26. Shahrajabian, M.H.; Cheng, Q.; Sun, W.N. The effects of amino acids, phenols and protein hydrolysates as biostimulants on sustainable crop production and alleviated stress. *Recent Pat. Biotechnol.* **2022**, *16*, 319–328. [CrossRef]
27. Fan, N.N.; Su, L.T.; Lv, A.M.; Wen, W.W.; Gao, L.; You, X.K.; Zhou, P.; An, Y. PECTIN ACETYLESTERASE12 regulates shoot branching via acetic acid and auxin accumulation in alfalfa shoots. *Plant Physiol.* **2024**, *195*, 518–533. [CrossRef] [PubMed]
28. Dwisandi, R.F.; Miranti, M.; Widiastuti, A.; Prismantoro, D.; Awal, M.A.; Mispan, M.S.; Joshi, R.C.; Doni, F. Microbial secondary metabolites for modulating plant biotic stress resistance: Bridging the lab-field gap. *Plant Stress* **2025**, *15*, 100720. [CrossRef]
29. Gharib, F.A.E.L.; Osama, K.; Sattar, A.M.A.E. Impact of *Chlorella vulgaris*, *Nannochloropsis salina*, and *Arthrospira platensis* as bio-stimulants on common bean plant growth, yield and antioxidant capacity. *Sci. Rep.* **2024**, *14*, 1398. [CrossRef]
30. Zhao, L.P.; Xiong, Y.; Zhang, P.; Zhang, P.; Sun, M.M.; Yang, L.; Shang, X.C.; Yu, T. Polysaccharides from *Ulva prolifera* promote tobacco plant growth by benefiting rhizosphere bacterial community in acidic soil. *Ind. Crops Prod.* **2025**, *234*, 121495. [CrossRef]
31. Cheng, C.; Steinman, A.D.; Xue, Q.J.; Xiang, W.; Xie, L.Q. The disruption of calcium and hydrogen ion homeostasis of submerged macrophyte *Vallisneria natans* (Lour.) Hara caused by microcystin-LR. *Aquat. Toxicol.* **2023**, *254*, 106377. [CrossRef] [PubMed]
32. Gao, F.; Guo, J.X.; Shen, Y.Y. Advances from chlorophyll biosynthesis to photosynthetic adaptation, evolution and signaling. *Plant Stress* **2024**, *12*, 100470. [CrossRef]
33. Cheng, C.; Steinman, A.D.; Xue, Q.J.; Zhang, L.; Xie, L.Q. The osmotic stress of *Vallisneria natans* (Lour.) Hara leaves originating from the disruption of calcium and potassium homeostasis caused by MC-LR. *Water Res.* **2023**, *245*, 120575. [CrossRef]

34. Li, C.; Chang, Y.; Luo, Y. Nitrogen regulates stem lodging resistance by breaking the balance of photosynthetic carbon allocation in wheat. *Field Crops Res.* **2023**, *296*, 108908. [CrossRef]
35. Nobre, B.P.; Villalobos, F.; Barragán, B.E.; Oliveira, A.C.; Batista, A.P.; Marques, P.A.S.S.; Mendes, R.L.; Sovová, H.; Palavra, A.F.; Gouveia, L. A biorefinery from *Nannochloropsis* sp. Microalga—Extraction of oils and pigments. Production of biohydrogen from the leftover biomass. *Bioresour. Technol.* **2013**, *135*, 128–136. [CrossRef]
36. Panis, G.; Carreon, J.R. Commercial astaxanthin production derived by green alga *Haematococcus pluvialis*: A microalgae process model and a techno-economic assessment all through production line. *Algal Res.* **2016**, *18*, 175–190. [CrossRef]
37. Torres, G.F.; Bermejo-Padilla, E.; Pittman, J.; Theodoropoulos, C. *Microalgae Strain Catalogue: A Strain Selection Guide for Microalgae Users: Cultivation and Chemical Characteristics for High Added-Value Products*; Zenodo: Geneva, Switzerland, 2021. [CrossRef]
38. David, Q.; Jonah, M.G.; Braden, J.L.; Jason, C.Q. Global Life Cycle and Techno-Economic Assessment of Algal-Based Biofuels. *Environ. Sci. Technol.* **2023**, *57*, 10.1021.
39. LI, J.; Hao, X.D.; Gan, W.; van Loosdrecht, M.C.M.; Wu, Y.U. Recovery of extracellular biopolymers from conventional activated sludge: Potential, characteristics and limitation. *Water Res.* **2021**, *205*, 117706. [CrossRef]
40. Nuohua, T.B.; Wilfert, P.; Eustace, S.J.; Korvingm, L.; van Loosdrecht, M.C.M. Phosphorous speciation in EPS extracted from Aerobic Granular Sludge. *Water Res.* **2024**, *262*, 122077. [CrossRef]
41. Wang, L.X.; Lei, Z.; Zhang, Z.X.; Yang, X.H.; Chen, R. Deciphering the role of extracellular polymeric substances in the adsorption and biotransformation of organic micropollutants during anaerobic wastewater treatment. *Water Res.* **2024**, *257*, 121718. [CrossRef]
42. Ben, H.H.; Mainardis, M.; Moretti, A.; Toye, D.; Léonard, A. Extracellular polymeric substances (EPS) in sewage sludge management: A call for methodological standardization. *J. Environ. Manag.* **2025**, *376*, 124407. [CrossRef]

Disclaimer/Publisher's Note: The statements, opinions and data contained in all publications are solely those of the individual author(s) and contributor(s) and not of MDPI and/or the editor(s). MDPI and/or the editor(s) disclaim responsibility for any injury to people or property resulting from any ideas, methods, instructions or products referred to in the content.